IEEE Open Access Journal of
Power and Energy

Received 22 October 2020; revised 31 March 2021; accepted 25 May 2021.
Date of publication 2 June 2021; date of current version 8 June 2021.

Digital Object Identifier 10.1109/OAJPE.2021.3084577

Quantifying Power System Operational and Infrastructural Resilience Under Extreme Conditions Within a Water-Energy Nexus Framework

SCOTT ZULOAGA [1] (Member, IEEE), AND VIJAY VITTAL [2] (Life Fellow, IEEE)

[1]Electrical Reliability Council of Texas, Taylor, TX 76574 USA
[2]School of Electrical, Computer, and Energy Engineering, Arizona State University, Tempe, AZ 85281 USA
CORRESPONDING AUTHOR: V. VITTAL (vijay.vittal@asu.edu)

This work was supported in part by the U.S. National Science Foundation (NSF) Project 029013-0010 (CRISP Type 2) - Resilient Cyber-Enabled Electric Energy and Water Infrastructures: Modeling and Control under Extreme Mega Drought Scenarios, and in part by the National Science Foundation Graduate Research Fellowship Program under Grant 026257-001.

ABSTRACT This work presents definitions and metrics developed for quantifying the resilience of the electric power system (EPS) while considering its interdependent operation with the water distribution system (WDS). These metrics are used within a novel formulation in order to determine EPS resilience during the coordinated real-time operation of the two systems where both the operational state and infrastructural configuration of the EPS is taken into account. Coordinated operation of the two systems involves simulations that account for the main dependencies of each system on the other (cooling water for thermoelectric generation and electric power for WDS pumps). The results for several test cases are used within this work to demonstrate how system resilience in the EPS is captured for simulations that emulate the critical conditions of long-term power outages (in the EPS) and severe drought (in the WDS).

INDEX TERMS Electric power system, extended time-period simulations, interdependent infrastructure systems, power system infrastructural resilience, power system operational resilience, water distribution system, water-energy nexus.

NOMENCLATURE

$dAdj_{xf,n,t}$	Load reduction amount, $xf \in \{sf, mf\}$, bus n, time t, from consumer survey results
EPS	Electric power system
$G_{TP,g}$	Generator type, generator g
HCF_g	Historical capacity factor, generator g
$LOL_{n,t}$	Loss of load, bus n, time-period t
mf_n	Fraction of multi-family (mf) homes in residential component of load, bus n
$P_{g,max}$	Maximum active power output, generator g
$P_{l,max}$	Rate A MVA limit, transmission element l
$P_{l,t}$	Active power flow, transmission element l, time-period t
$P_{load,nt}$	Active power demand, bus n, time-period t
sf_n	Fraction of single-family (sf) homes in residential component of load at bus n
sl	Transmission line index function calculation parameter, summing length
TLg, t	Cooling water storage tank level, generator g, time-period t
WDS	Water distribution system

Index Functions:

R^g_{CW}	Cooling water index function, generator g
R^n_{DS}	Overall demand supplied index function, bus n
R^n_{PL}	WDS pump load supplied index function, bus n
R^l_{TL}	Transmission line thermal limit index function, branch l
R^n_V	Voltage index function, bus n

Operational Resilience Measures of Performance (RMP):

$Res_{R^n_V,t}$	RMP for voltage, time-period t
$Res_{R^l_{TL},t}$	RMP for transmission lines, time-period t
$Res_{R^g_{CW},t}$	RMP for cooling water supply, time-period t

$Res_{R^n_{DS},t}$	RMP for overall demand supplied, time-period t
$Res_{R^n_{PL},t}$	RMP for WDS pump demand supplied, time-period t
$Res_{EPS,TOT}(t)$	Overall EPS operational resilience at time t

Infrastructural Robustness Metrics (IRM):

$M_{ED,n}$	EPS connectivity IRM for bus n
$M_{EB,l}$	EPS betweenness IRM for element l
$M_{EFF,n}$	EPS efficiency IRM for bus n
$M_{SCW,g}$	EPS generator cooling water significance IRM for generator g

IOR Functions:

$R_{R^n_V,t}$	Final resilience value for voltage, IOR based calculation, time t
$R_{R^l_{TL},t}$	Final resilience value for transmission elements, IOR based calculation, time t
$R_{R^n_{DS},t}$	Final resilience value for overall demand satisfied, IOR based calculation, time t
$R_{R^n_{PL},t}$	Final resilience value for pump demand supplied, IOR based calculation, time t
$R_{R^g_{CW},t}$	Final resilience value for thermoelectric generators, IOR based calculation, time t

Total IOR Values:

$R_{TOT}(t)$	Combined EPS IOR measure of performance
$Res_{EPS,IND}$	EPS independent IOR terms: voltage, transmission line, overall load supplied
$Res_{EPS,INTR}$	EPS interdependent IOR terms: thermoelectric cooling water supplied and WDS pump load supplied

Weights:

w_1, w_2	Weights associated with the independent and interdependent terms, respectively, for IOR
w_v, w_{tl}, w_{cw}, w_{ds}, w_{pl}	Weights associated with voltage, Transmission element, cooling water, overall demand supplied and WDS pump demand supplied terms, respectively, for EPS IOR

I. INTRODUCTION

THE electric power system (EPS) and the water distribution system (WDS) comprise what is informally referred to as the water-energy nexus. This is due to the fact that the systems have several interdependencies [1], [2] which have been known for some time and which have garnered more attention in recent years. This interest has coincided with interest in the more general and broader domain of critical interdependent systems. The authors in [3] have provided definitions and different types of dependencies which can exist between interdependent infrastructure systems as well as a general procedure for data collection and analysis of such systems. Another broad examination of interdependent systems, their behaviors, points of failures, and operation is detailed in [4].

With regards to the water-energy nexus, it is noted that the main interdependency of the EPS on the WDS is cooling water for thermoelectric generation [5]. Although water is used in several processes at thermoelectric generation plants, the water used for the cooling cycle is estimated to be about 90% of a plant's total water consumption [6]. Further, the main need for electricity in the WDS is for powering pumping stations for water delivery and storage [7] with the authors in [8] summarizing that water distribution pumping typically composes about 67% of a water utility's total energy consumption. There have been many water related-electric generation issues due to both water shortages and high-temperatures which have been documented throughout the US [11]. Another area of concern is the possibility of the occurrence of high-impact, low-probability events. In the study area of interest (American Southwest), an example of such an event is evidenced by the possibility of a mega-drought [12] which can have detrimental effects on the water and energy systems [13] and far beyond.

As more stress is placed upon interdependent systems due to factors such as increased demand, outages, or even natural events, it is becoming ever more important to study the impacts that each system has upon the other. The water, energy, and food systems are studied using a system of systems approach in [9] where a high-level overview of how the water, energy and food systems interact with each other and insights on how this knowledge can be useful in making future policy is presented. A multi-energy systems framework considering electric, gas, heating and water systems is presented in [10], where the authors model the coupling of the various systems to each other and study the coordinated operation of the systems under various short-term scenarios.

Just as the water-energy nexus is now receiving more attention, the area of resilience for critical infrastructure systems has had more focus directed towards it. The National Infrastructure Advisory Council (NIAC) presents what the authors call the *NIAC resilience construct* which is based on the four concepts of *robustness, resourcefulness, rapid recovery, and adaptability* [14]. The authors in [15] describe the obvious economic advantages of having an electric system which is resilient to weather conditions by detailing the impact that weather related grid issues cause and also discuss strategies to help mitigate this risk. An overview of quantifying resilience in various field is presented in [16], while a methodology for the quantitative assessment of the resilience of interdependent systems is given in [17].

Efforts to quantify and examine various aspects of WDS resilience are explored in [18]–[20], with [19] investigating quantitative resilience definitions and the authors in [20] presenting a computation methodology for calculating WDS operational resilience. Several works have considered power

system resilience in the face of different natural disasters and other low probability, extreme events. In [21], the authors present an overview of EPS outage forecasting, examples of efforts to increase system resilience to events by the hardening of various components and a brief discussion on infrastructure interdependencies with a main focus on the gas and electric networks. References [22] and [23] both provide a comprehensive look at resilience from a power system perspective and offer details of extreme events, reviews of resilience definitions, expected performance of resilience metrics during disturbances and how to quantify those metrics, and both references summarize potential options for improving system resilience in the future. Lastly, the main author in [24]–[26] has presented several recent works on both quantifying resilience and assessing power system resilience in scenarios with extreme windstorms.

As resilience is a loosely defined term, this work seeks to help eliminate some ambiguity by presenting a rigorous, mathematical formulation for the purpose of a system level resilience calculation. This formulation then allows for assessments of system resilience using metrics such as the ones in [17]. The remaining sections of this paper are organized as follows. Section II presents the definitions of terms used in quantifying resilience and the formulation of the resilience metrics. Section III describes the simulation setup, the scenarios, and the test cases used in this work. A discussion of the results of the simulations performed is in Section IV and the conclusion is in Section V.

II. EPS RESILIENCE METRICS

The aim of the metrics proposed in this section is to facilitate the resilience calculation of the system under consideration, given the quantities available from the simulations that were performed and such that the framework discussed in the section above can be used to quantify this resilience. The definitions for four terms used extensively in the following section will now be provided. The starting point for all of the resilience calculations is the *index function*. This function aims to relate the values of operational parameters (e.g. a bus voltage) to how that quantity affects overall system performance. The next step is to use the values calculated from the index functions to obtain the *resilience measure of performance* (RMP), which can be viewed as a metric of the measure of resilience. The expected behavior of such a metric before, during and post-disturbance is illustrated in, for example, [16] and [17]. Lastly, there are the *infrastructural robustness metrics* (IRM), which are used in order to determine a weight for each RMP in preparation for its inclusion in the final *infrastructural-operational resilience* (IOR) measure. For example, the voltage RMP in a given time period will be calculated as the sum of all of the bus voltage RMPs. However, it is likely that not all of the buses within the system are equally important to the system's operation or integrity and therefore the contribution of some bus voltage values to the overall resilience value should be less as compared with other buses.

The IRMs therefore provide a systematic means of weighting the RMPs to offer a more complete view of system resilience since both the system operating conditions as well as the system network topology are taken into consideration for the total resilience value. Although the above example considered the EPS voltage RMP, the same logic can easily be extended to the other operational resilience metrics.

The following sub-sections present the mathematical formulation for the index functions and final IOR measures of performance as well as a brief description of each. Further details and a more in-depth discussion of the formulation for RMPs and IOR can be found in [27], [28]. The notation system builds on itself as one goes from index functions to the RMPs and finally to the IORs. The index functions are all subscripted with an abbreviation reflecting the corresponding system quantities that are used for calculation. The RMP and IOR function notations are then subscripted with the appropriate index function notation to clarify the associated quantities that are being referenced.

A. OPERATIONAL RESILIENCE METRICS

1) VOLTAGE INDEX FUNCTION

It is desired for the voltage magnitudes in the EPS to be kept within certain ranges, both in steady-state operation and following the occurrence of system disturbances. The reason for this is that system performance can degrade as voltages deviate from their nominal values, so the bus voltage index function captures this degradation by maintaining its maximum value (one) for the voltage range of 0.975 pu – 1.025 pu. This value then linearly approaches zero at 0.9 pu (1.1 pu) as the voltage decreases (increases). These values can be adjusted according to a specific planning guide, such as the 0.95-1.05 pu steady-state and 0.9-1.05 pu post-contingency voltage ranges given in [29]. A piece-wise linear function which demonstrates the behavior described above is summarized mathematically as:

$$R_V^n = \begin{cases} 0 & V_n < V_{min} \\ 13.\bar{3} \cdot V_n - 12 & V_{min} \leq V_n \leq V_{thr,min} \\ 1 & V_{thr,min} \leq V_n \leq V_{thr,max} \\ -13.\bar{3} \cdot V_n + 14.\bar{6} & V_{thr,max} \leq V_n \leq V_{max} \\ 0 & V_{max} < V_n \end{cases} \quad (1)$$

where V_n is the bus voltage magnitude in pu and the parameters $V_{thr,min/max}$ and $V_{min/max}$ are the values where R_V^n starts decreasing and the values where it reaches zero, respectively, as described above. The values of $13.\bar{3}$, 12, and $14.\bar{6}$ are due to the numerical values chosen for $V_{thr,min/max}$ and $V_{min/max}$ and where, for completeness, $13.333\ldots = 13.\bar{3}$ and $14.666\ldots = 14.\bar{6}$.

2) TRANSMISSION LINE INDEX FUNCTION

System performance is also dependent on the flows through transmission line elements. However, transmission elements have several separate ratings corresponding to the maximum power flow magnitudes and the amount of time for which

the element can be operated at that MVA level. The index function is formulated with this constraint in mind and instead of the index function value being based on the instantaneous line flow magnitude at a given time, it is based on an averaged flow value. The planner or operator performing this study then has the flexibility to adjust the summing length parameter, *sl*, in order to make the index function value more or less sensitive to temporary line flows exceeding the Rate A (steady-state) MVA limit of the equipment. The index function is given as:

$$R^{l}_{TL} = min\left(1, \frac{P_{l,max} \cdot sl}{\sum_{r=t-sl}^{t-1} P_{l,r}}\right) \tag{2}$$

where $P_{l,max}$ is the Rate A MVA line limit and $P_{l,r}$ is the line flow in time-period *r*.

3) LOAD SUPPLIED INDEX FUNCTIONS

Two index functions are presented for quantifying system performance with regards to loads in the EPS. The first leverages knowledge of consumer information to develop a generic load supplied metric and the other is for WDS pump loads and is scenario dependent.

For the types of extreme events studied in this work, it is known [30] that consumers are willing to change their consumption of both water and electricity. The consumers have been shown to have slightly different amounts of willingness to change their consumption based on their knowledge of dependencies between the EPS and WDS as well as whether the curtailment of water and energy usage is mandatory. The bus loads in the EPS are therefore decomposed into representative percentages for industrial, commercial and residential components within the simulation to account for this fact within this resilience calculation. This can be used to determine if the net load served in a given time period is less than what might need to be served if consumers had decreased their demand given the extreme scenario. The index function assumes a value of 0 if this is the case and a value of 1 if not. Denoting a percentage of the total load ($P_{load,nt}$) at bus n in time-period t as single-family (sf_n) and another percentage as multi-family (mf_n), the demand adjustment factors ($dAdj_{sf,t}$, $dAdj_{mf,t}$) and any loss of load ($LOL_{n,t}$) in the simulation can then be used to formulate the load supplied (overall) index function as:

$$\begin{aligned} R^{n}_{DS} &= ceil\left(\begin{array}{l}\left(P_{load,nt} - LOL_{n,t}\right) - \\ \left(P_{load,nt} - sf_n \cdot dAdj_{sf,t} - mf_n \cdot dAdj_{mf,t}\right)\end{array}\right) \\ &= ceil\left(sf_n \cdot dAdj_{sf,t} + mf_n \cdot dAdj_{mf,t} - LOL_{n,t}\right) \end{aligned} \tag{3}$$

Outages for the WDS pumps in the system were pre-specified as a part of the scenario definition. An index function based on these outages and the output from the WDS pump schedule optimization was used to compute a value of zero or one based on whether the pump was scheduled during an outage hour. The load supplied (WDS pumps) index function is expressed as:

$$R^{n}_{PL} = \begin{cases} 1, & PL_{demand} = PL_{supply} \\ 0, & PL_{demand} > PL_{supply} \end{cases} \tag{4}$$

where PL_{demand} is the active power demand as determined from the WDS network solution and PL_{supply} is the value given by the scenario definition and where $PL_{demand} = PL_{supply}$ during time-periods with no contingency.

4) THERMOELECTRIC COOLING WATER INDEX FUNCTIONS

The main usage of water for thermoelectric generation plants is for the cooling cycle where water is used in the process of converting the heated working fluid from steam back to liquid via heat transfer. The cooling cycle can be an open or closed cycle, with the latter exemplified by power plants using cooling towers. The use of cooling towers introduces losses through drift, blowdown and evaporation and the water needed to replenish the amount which is lost represents the key dependency of the EPS on the WDS. Since the amount of onsite storage for cooling water is normally substantial, it is reasonable to assume that the onsite tank levels will not change vary rapidly either under normal conditions or even when operating under sub-optimal conditions related to the re-supply of cooling water that is consumed. Given the substantial storage and the slow rate of change in that storage, the system will be able to function at a satisfactory level even with changes in the level of onsite water storage. The index function used for thermoelectric cooling water changes slowly with respect to time to reflect this fact and tracks the tank level via a piece-wise linear step function:

$$R^{g}_{CW} = \frac{ceil\left(\frac{TL_{g,t}}{TL_{g,initial}} \cdot 10\right)}{10} \tag{5}$$

where $TL_{g,t}$ is the tank level at time t and the initial tank level is $TL_{g,initial}$.

B. RESILIENCE MEASURE OF PERFORMANCE DEFINITION

The resilience measure of performance formulation is based on that given in [31] and is stated in words here as:

$$\begin{aligned} &Res_{f,t} \\ &= \frac{\#\ of\ \ times\ satisfactory\ operation\ follows\ unsatisfactory}{\#\ of\ \ times\ \ unsatisfactory\ operation\ occurs} \end{aligned} \tag{6}$$

Unsatisfactory operation is defined as the resilience index function value being less than that function's value in the previous simulation hour and satisfactory operation is denoted by an increase in the index function's value. For the interdependent infrastructure metrics, a more restrictive definition of unsatisfactory operation in a given time-period is defined. For those cases, if the index function is less than its maximum value of 1, this is considered unsatisfactory. The RMPs are defined as real values between 0 and 1.

C. INFRASTRUCTURAL RESILIENCE METRICS

Three IRMs based on graph theory principles and detailed in [32], [33] were uniquely applied as weights to the RMPs in [28]. These metrics were:

1) Bus importance metric ($M_{ED,n}$, *degree*)
2) Branch importance metric ($M_{EB,l}$, *betweenness*)
3) Load importance metric ($M_{EFF,n}$, *efficiency*)

A new metric that was used to determine the importance of the cooling requirements of thermoelectric generators within the system is now presented.

4) Thermoelectric generator importance metric

This metric combines the generator's type (base-load (*bl*), load-following (*lf*), peaking (*pk*)), contribution to system generation capacity, and the unit's historical capacity factor [34]. The importance factor characterizing the significance of cooling water supplied to generator g is expressed as the sum of these values:

$$M_{SCW,g} = G_{TP,g} + \frac{P_{g,max}}{\sum_j P_{j,max}} + HCF_g \tag{7}$$

These quantities are relevant to ensuring grid integrity because base-load units are: 1) typically less efficient (resulting in higher water consumptions/withdrawals) 2) supply a large amount of the electrical energy 3) are in continuous operation for long periods of time. Values of $G_{TP,g}$ for individual units can be a pre-determined default value (see Tables 1 and 2) or another specific value as the planner or operator sees fit. It is noted here that all of the IRMs were normalized for use in calculating IOR values.

TABLE 1. Generator fuel types – 14 bus system.

Generator Fuel Type	Generator Bus	Generator Type (Value)
CF	1	*bl* (1)
Npp	2	*bl* (1)
CT	3	pk (0.5)
CT	6	*pk* (0.5)
CCGT	8	*lf* (0.75)

TABLE 2. Generator fuel types – RTS 96 system.

Generator P_{max} (MW)	Generator Fuel Type	Generator Type (Value)
100, 155, 197, 350	CF	*lf* (0.75), *bl* (1), *bl, bl, bl*
400	Npp	*bl*
12, 20	CT	*pk*
50	Hydro	-
76	CCGT	*lf* (0.75)

D. IOR

Weighting the appropriate RMP by the corresponding IRM gives the final formulation for each IOR quantity. The general form of each expression is the weight multiplied by the RMP, where (6) is written explicitly in terms of an index function. The extensive form of the IRM in (8)-(11) can be seen in [28].

1) VOLTAGE IOR

The IOR value for bus voltages is calculated by weighting the RMP for voltages with the degree IRM:

$$R_{R_V^n,t} = \left(\sum_{n=1}^{NB} M_{ED,n} \cdot max(0, R_V^n(t) - R_V^n(t-1))\right) / \left(\sum_{n=1}^{NB} ceil(R_V^n(t-1) - R_V^n(t))\right) \tag{8}$$

2) TRANSMISSION LINE IOR

The IOR value for transmission line thermal limit resilience is calculated by using the betweenness IRM to weight each branch's operational thermal limit resilience:

$$R_{R_{TL}^l,t} = \left(\sum_{l=1}^{NL} M_{EB,l} \cdot max(0, R_{TL}^l(t) - R_{TL}^l(t-1))\right) / \left(\sum_{l=1}^{NL} ceil(R_{TL}^l(t-1) - R_{TL}^l(t))\right) \tag{9}$$

3) LOAD SUPPLIED IOR

The load supplied IOR values are calculated by weighting the RMP for load supplied (overall) and the load supplied (WDS pumps) with the efficiency IRM:

$$R_{R_{DS}^n,t} = \left(\sum_{n=1}^{NBL} M_{EFF,n} \cdot max(0, R_{DS}^n(t) - R_{DS}^n(t-1))\right) / \left(\sum_{n=1}^{NBL} ceil(R_{DS}^n(t-1) - R_{DS}^n(t))\right) \tag{10}$$

$$R_{R_{PL}^n,t} = \left(\sum_{n=1}^{NPL} M_{EFF,n} \cdot max(0, R_{PL}^n(t) - R_{PL}^n(t-1))\right) / \left(\sum_{n=1}^{NPL} ceil(1 - R_{PL}^n(t))\right) \tag{11}$$

4) THERMOELECTRIC GENERATION IOR

The IOR values for thermoelectric generation are calculated by weighting the RMP for thermoelectric generation cooling water by the thermoelectric generator importance metric:

$$R_{R_{CW}^g,t} = \left(\sum_{g=1}^{NG} \left(G_{TP,g} + \frac{P_{g,max}}{\sum_j P_{j,max}} + HCF_g\right) \cdot max(0, R_{CW}^g(t) - R_{CW}^g(t-1))\right) / \left(\sum_{g=1}^{NG} ceil(1 - R_{CW}^g(t))\right) \tag{12}$$

Here it is explicitly noted again that the two IOR expressions involving interdependent system quantities (WDS pump load supplied and thermoelectric generation) have a stricter enforcement on unsatisfactory operation as any value less than 1 is considered unsatisfactory.

5) TOTAL IOR

The final value of IOR is expressed as the weighted sum of (8)-(12):

$$\mathrm{R_{EPS,TOT}}(t) = \left(\begin{matrix} w_v R_{R_V^n,t} + w_{tl} R_{R_{TL}^l,t} + w_{cw} R_{R_{CW}^g,t} \\ + w_{ds} R_{R_{DS}^n,t} + w_{pl} R_{R_{PL}^n,t} \end{matrix}\right) / \left(w_v + w_{tl} + w_{cw} + w_{ds} + w_{pl}\right) \tag{13}$$

which, for convenience, can be expressed in terms of the independent and interdependent system quantities in order to examine the impact of the independent and interdependent quantities on the overall resilience calculation in the results section:

$$R_{EPS,TOT}(t) = f(Res_{EPS,IND}) + f(Res_{EPS,INTR}) = \left(\begin{matrix} w_1 \left(R^n_{V},t + R_{R^l_{TL},t} + R_{R^n_{DS},t} \right) \\ +w_2 \left(R_{R^g_{CW},t} + R_{R^n_{PL},t} \right) \end{matrix} \right) / w_3 \quad (14)$$

A flow chart showing the IOR calculation methodology is shown in Fig. 1. The selection of a value to be used as a weight for a particular term depends both on the relative importance of the term as well as the magnitude of the expected values of the term. While it is not clear that there are values for the weights that are applicable or desirable for all study scenarios, the presented formulation gives some flexibility to highlight particular quantities based on the study scenario.

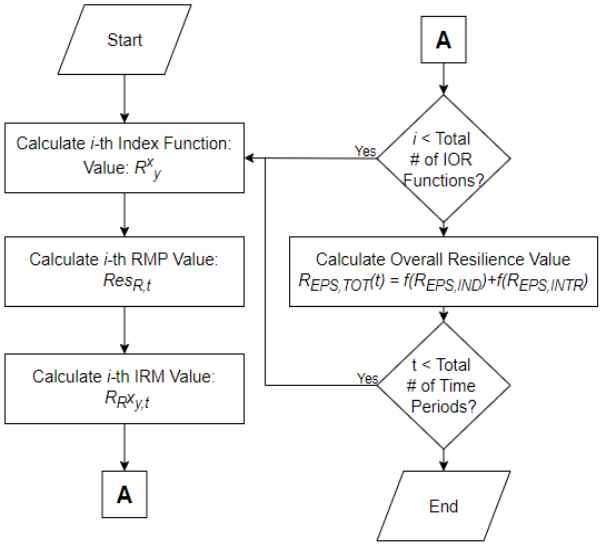

FIGURE 1. **IOR computation methodology flow-chart.**

III. TEST CASES, SIMULATION DESCRIPTION AND SCENARIOS

A. TEST SYSTEMS

Results will be shown for simulation scenarios run using two different test systems. The first was a modified version of the IEEE 14-bus test system [35]. In order to include the representation of the WDS, two representative distribution systems [36] were added to the nominal test system. These reflect the inclusion of pumping stations for both a freshwater source and a wastewater treatment plant. The WDS commercial and residential demands are supplied by the freshwater source while both sources are used to supply the generation stations which have cooling water requirements (thermoelectric). Fig. 2 shows the physical interdependencies of the EPS and WDS as WDS pumps are modeled as loads in the EPS and

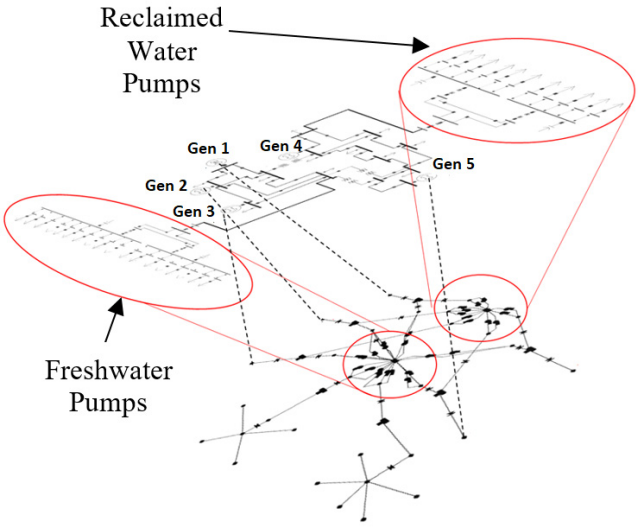

FIGURE 2. **Modified IEEE 14 bus test system and test WDS.**

generator cooling water demands are shown (mapping shown via dashed lines) as node demands in the WDS.

The second test system is the 73-bus RTS-96 system [37] where the three areas within the system are shown explicitly in Fig. 3. In order to calculate cooling water requirements for the thermoelectric units within the two systems, historical consumption rates which relate a unit's power produced to

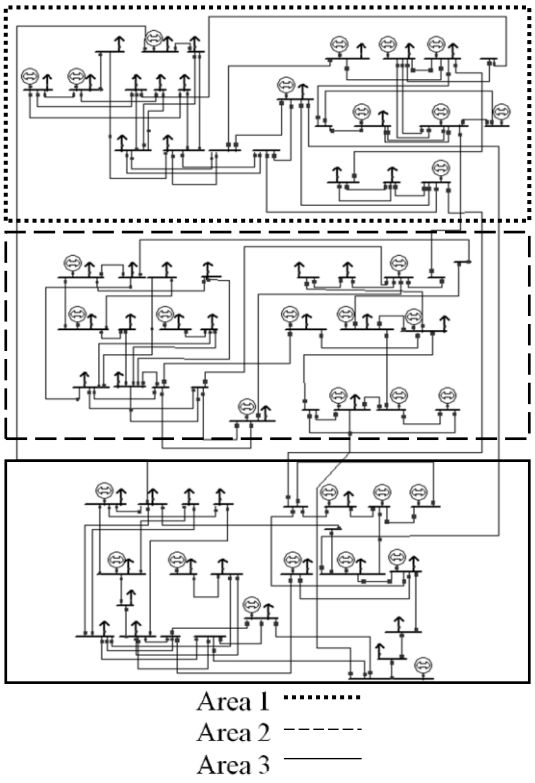

FIGURE 3. **Three area RTS96 test system.**

the water it consumes were utilized. Also required for various calculations is the specification of the fuel type [38] for each of the thermoelectric plants and the $G_{TP,g}$ value. This information is summarized in Table 1 and Table 2 for the 14-bus and 73-bus systems, respectively.

B. SIMULATION DESCRIPTION

A framework and methodology for the extended period simulation and optimization of operations of the EPS and WDS under extreme conditions has been presented by the authors in [38]. This framework consisted, in part, of the development of a simulation engine which performs extended time-period simulations and the coordinated optimization of the EPS and WDS. Using this engine, a scenario of extreme conditions was simulated using the modified 14-bus system. The extreme conditions consisted of time-periods during the simulation where the total water available within the WDS was limited, thus emulating a drought, and time-periods of extended electric power outages affecting some WDS pumps. The results from the simulation were then utilized for that system's resilience calculations. The motivation for this scenario arises from the fact that non-gravity based WDSs need electricity for pumping to remain operable just as conventional thermoelectric generation requires cooling water to remain operable.

For the 73-bus system, the following methodology was used. First, it was assumed that one scaled version of the WDS test system developed for use with the 14-bus system could supply one (of the three) areas within the RTS96 system. Then, the amount of cooling water that was supplied over the course of the initial simulation to each generator was divided by the cooling water actually requested by that generator. This was done in order to determine the amount supplied as a percentage of that which was requested and in effect this gives a per-unit value of demand satisfied which could be used for simulations with this test system. For each generator within the drought hit area, these pu values were used as the amount of cooling water supplied to the respective thermoelectric fuel type within this larger system. The cooling water supplied to units not in the drought hit area as well as to all hydro units was assumed to equal to whatever was requested for the purpose of the larger system simulation scenarios.

IV. RESULTS DISCUSSION

The plots in Fig. 4 show the components of the total resilience calculation in terms of the independent and interdependent IOR quantities. As can be seen, the resilience value of the independent IOR quantities degrades as the simulation progresses due to increased loading as well as the outages that occur. The interdependent value steadily decreases as the water shortages in the WDS take place and the value is also affected by the WDS pump outages which occur intermittently throughout the simulation.

Fig. 5 shows a comparison of the final IOR values in the 14-bus system with different values for the weight on interdependent quantities (w_2 in (14), with w_1 being equal to

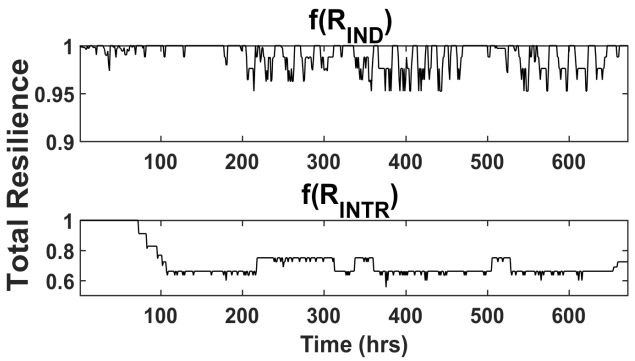

FIGURE 4. Independent and interdependent system quantity IOR values.

unity). The main takeaways are as follows. First, the IOR formulation captures the scenario definition in that the resilience value begins decreasing as the electric power outages are placed on the system and the effects of the water-shortage begin to propagate from the WDS to the EPS. Then there are periods of increased resilience as these disturbances are cycled throughout the simulation, and the resilience begins to recover at the end of the simulation as expected. Second, with $f(Res_{EPS,INTR})$ weights being 1 and in comparison with the results in [27], the larger fluctuations in the magnitude of overall IOR can be attributed to more important $f(Res_{EPS,IND})$ quantities having a larger impact due to the increased importance given to them by their IRMs. Thirdly, the decrease in the magnitude of those fluctuations and the smaller decrease in the overall resilience values as w_2 goes from five to twenty-five as compared with the change from one to five shows that the resilience value becomes dominated by the interdependent system quantities.

Fig. 6 shows the results for the drought/outage scenario applied to one of the three areas in the 73-bus system. Highlighted here is the effect of including the IRMs on the final resilience value. This effect is noted as more clearly emphasizing both the slow fluctuations in resilience value due to interdependent system quantities as well as an increased magnitude in the higher-frequency fluctuations, which is the result of changing bus voltages and line flows. Fig. 7 gives insight into how this decrease in the magnitude of the resilience value occurs with the inclusion of the IRMs. Shown in this plot are the onsite storage levels for 10 generators within the drought area and it is noted that Unit 89 experiences a significant drop in its tank level. Given that this is a baseload unit, its $M_{SCW,g}$ value will be much greater than a peaking unit, since it has both a larger $G_{TP,g}$ value as well as HCF_g value. Thus, the drop in this tank level will contribute relatively more to the overall decrease in magnitude of the cooling water IOR and therefore the final IOR value as well.

Following the desire to extend the operation of plants in areas experiencing extreme drought for as long as possible, the dispatch of generation was changed via a parameter value alteration, $\delta_{fuelCost}$, in the combined economic and

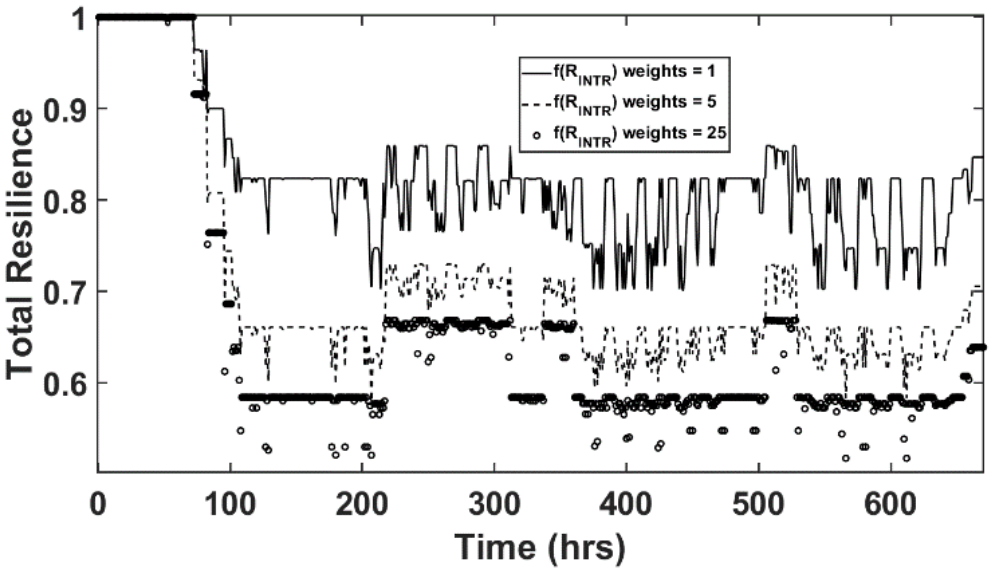

FIGURE 5. System resilience – interdependent quantity weight comparison – modified 14-bus system.

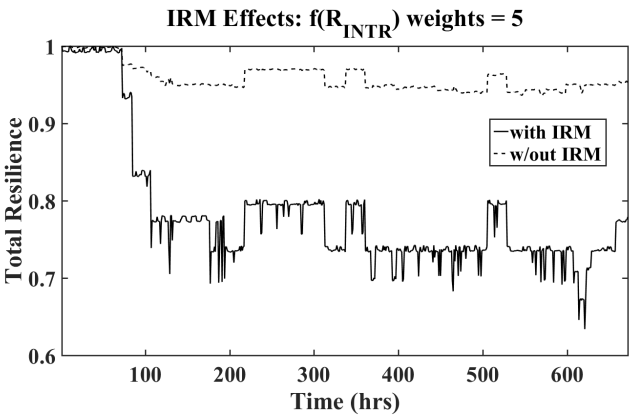

FIGURE 6. Impact of IRM inclusion – 73-bus system.

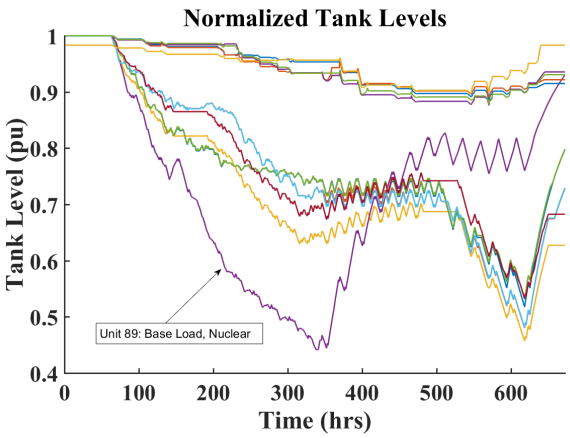

FIGURE 7. Normalized onsite water storage for generators supplied by WDS under drought conditions – 73 bus system.

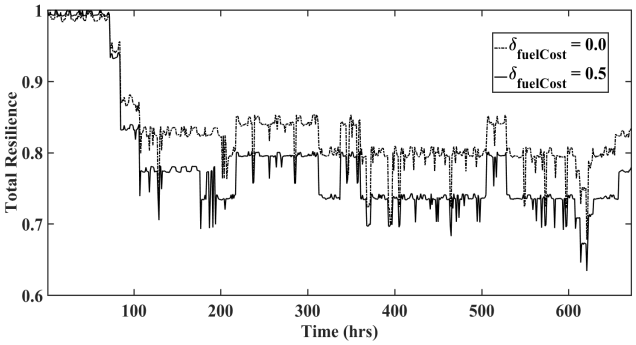

FIGURE 8. System resilience comparison for different dispatch priorities.

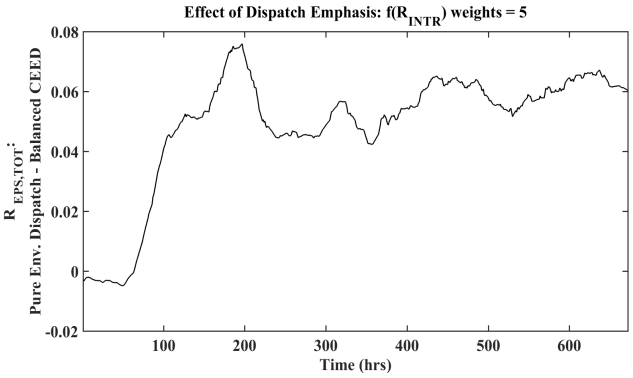

FIGURE 9. Difference of system resilience for different dispatch priorities.

environmental dispatch formulation developed in [30]. The effect of this change was to move the dispatch from one having balanced considerations for fuel and operational water costs to a pure environmental dispatch. Fig. 8 shows the system resilience value for the two cases and it is seen that an environmental dispatch does result in a higher system resilience value in most time-periods throughout the simulations. Fig. 9 shows a plot of the smoothed algebraic difference

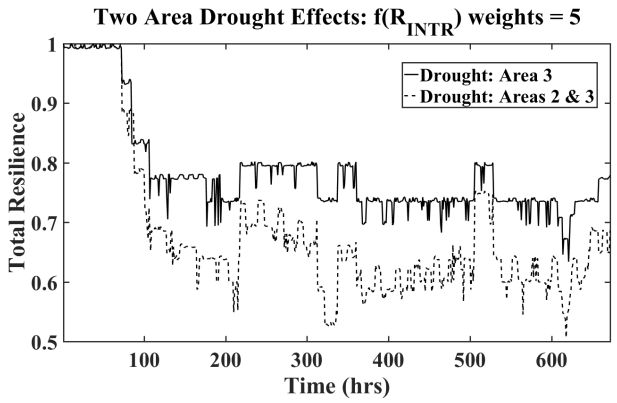

FIGURE 10. System resilience comparison for different generation dispatch priorities – 73 bus system.

in resilience values between the simulations having an environmental dispatch and one having a balanced dispatch (equal weight on fuel and operational water costs). As can be clearly seen, the improvement in the resilience value for the pure economic dispatch is evident with the positive value of the plot in this figure. At the beginning of the simulation, there are small fluctuations in this difference due to different operating conditions, but this difference grows larger in magnitude as the disturbances in the WDS and EPS system begin to occur. At the end of the simulation, this difference remains relatively constant, meaning the resilience values are increasing at approximately the same rate. The averaged improvement in system resilience over the course of the 28 day simulation is seen to be approximately 4.87 percent, proving that this is one possible way to both extend the operation of plants experiencing such conditions and in the process improve the overall system resilience value.

The last scenario to be considered is one where drought conditions are experienced in Areas 2 and 3 within the 73-bus system. Fig. 10 shows the plots that contrast the IOR value for the scenario of drought in only one area with this one. Here, the resilience value is lower overall during this system disturbance, as expected, and in addition to the decrease in system resilience during the drought periods attributed to the $R_{R^g_{CW},t}$ IOR term, the large decreases and increases in the total IOR that are due to the pump outages is more clearly seen.

It is noted here that the system level resilience value that is calculated with the proposed methodology can be further analyzed. Using metrics such as the ones presented in [17], the behavior of the system's resilience can be quantified directly in terms that relate to the four key concepts which are outlined in [14] and which are repeated here: robustness, resourcefulness, rapid recovery, and adaptability. This quantification thus brings the full picture into view and allows for the effect of various disturbances to be understood. The last concept listed, adaptability, represents a sort of feedback loop whereby it is desired that the resilience decreases in response to future disturbances be less severe. Along these lines, the improvement of resilience during simulation that was shown by altering the dispatch so further investigation into this and alternative ways to help ensure resilient system operation are representative of future work.

Lastly, the scalability of this methodology was examined by recording the computation times required to complete the post-simulation resilience calculations. The calculations were performed using MATLAB on a machine with a four core, 3.6 GHz i7 processor and the results are shown in Table 3. Given the short computation times needed to compute the final IOR value, this methodology seems suitable for both real-time and post-simulation analysis.

TABLE 3. Post-simulation resilience computation times.

Test System	IRM Calculation	Time (sec)
Modified 14 Bus	No	1.6431
73 Bus	No	2.5374
Modified 14 Bus	Yes	1.7412
73 Bus	Yes	3.2692

V. CONCLUSION

Conditions of limited water availability (such as droughts) and electric power outages are important factors which affect the performance of the EPS and WDS and the significance of such conditions are crucial to study given the interdependency between the two systems. This work presented a formulation for the calculation of power system resilience and a methodology for this calculation using operational measures of performance related to several quantities of interest with consideration of the EPSs interdependency with the WDS. The methodology was then extended with the use of infrastructural metrics that were used as weights for the operational resilience quantities.

The results from several scenarios on two different test systems were displayed in order to demonstrate the applicability of the presented calculation methodology and its ability to capture system operating conditions and topology configurations in the reflection of an overall system resilience calculation. The proposed methodology also incorporates several parameters and weights that allow for the planning or operating engineer to emphasize important topological elements in the study system as well as adjust the importance of independent or interdependent system quantities as the study scenario dictates.

The computational burden, as assessed by the post-simulation computation times, shows that this formulation and calculation methodology could be incorporated into a real-time assessment of the two systems. Further research will include the application of this methodology into a larger, realistic test-system in order to demonstrate its applicability in improving grid integrity over long periods of extreme, drought conditions and inclusion of feedback mechanisms in the system controls which seek to improve system resilience to future disturbances.

ACKNOWLEDGMENT

Any opinions, findings and conclusions or recommendations expressed in this material are those of the authors and do not necessarily reflect the views of the National Science Foundation.

REFERENCES

[1] N. Vakilifard, M. Anda, P. A. Bahri, and G. Ho, "The role of water-energy nexus in optimising water supply systems—Review of techniques and approaches," *Renew. Sustain. Energy Rev.*, vol. 82, pp. 1424–1432, Feb. 2018.

[2] S. Roy and L. Chen, "Water use for electricity generation and other sectors: Recent changes (1985-2005) and future projections (2005-2030)," EPRI, Palo Alto, CA, USA, Tech. Rep. 1023676, Nov. 2011.

[3] F. Petit *et al.*, "Analysis of critical infrastructure dependencies and interdependencies," Argonne Nat. Lab., Argonne, IL, USA, Tech. Rep. ANL/GSS-15/4, Jun. 2015.

[4] S. M. Rinaldi, J. P. Peerenboom, and T. K. Kelly, "Identifying, understanding, and analyzing critical infrastructure interdependencies," *IEEE Control Syst. Mag.*, vol. 21, no. 6, pp. 11–25, Dec. 2001.

[5] K. Gerdes and C. Nichols, "Water requirements for existing and emerging thermoelectric plant technologies," NETL, Golden, CO, USA, Tech. Rep. 402/080108, 2009.

[6] L. Badr, G. Boardman, and J. Bigger, "Review of water use in U.S. thermoelectric power plants," *J. Energy Eng.*, vol. 138, no. 4, pp. 246–257, Dec. 2012.

[7] *Integrated Energy Policy Report*, California Energy Commission, Sacramento, CA, USA, 2005.

[8] S. C. Jones and R. B. Sowby, "Quantifying energy use in the U.S. public water industry—A summary," *ASCE EWRI Currents*, vol. 16, no. 4, pp. 6–9, 2014.

[9] Y. Xiao, K. W. Hipel, and L. Fang, "A system of systems framework for the water-energy-food nexus," in *Proc. IEEE Int. Conf. Syst., Man Cybern. (SMC)*, Oct. 2019, pp. 994–999.

[10] C. Wang, N. Gao, J. Wang, N. Jia, T. Bi, and K. Martin, "Robust operation of a water-energy nexus: A multi-energy perspective," *IEEE Trans. Sustain. Energy*, vol. 11, no. 4, pp. 2698–2712, Oct. 2020.

[11] J. McCall, J. Macknick, and D. Hillman, "Water-related power plant curtailments: An overview of incidents and contributing factors," NREL, Golden, CO, USA, Tech. Rep. TP-6A20-67084, 2016.

[12] B. I. Cook, T. R. Ault, and J. E. Smerdon, "Unprecedented 21st century drought risk in the American Southwest and Central Plains," *Sci. Adv.*, vol. 1, no. 1, pp. 1–8, Feb. 2015.

[13] C. B. Harto *et al.*, "Analysis of drought impacts on electricity production in the Western and Texas interconnections of the United States," Argonne Nat. Lab., Argonne, IL, USA, Tech. Rep. ANL/EVS/R-11/14, Dec. 2011.

[14] A. R. Berkeley, III, and M. Wallace, "A framework for establishing critical infrastructure resilience goals: Final report and recommendations," Nat. Infrastruct. Advisory Council, DHS, Washington, DC, USA, Tech. Rep., Oct. 2010.

[15] *Economic Benefits of Increasing Electric Grid Resilience to Weather Outages*, Executive Office President, U.S. Dept. Energy's Office Electr. Del. Energy Rel. White House Office Sci. Technol., Washington, DC, USA, 2013.

[16] S. Hosseini, K. Barker, and J. E. Ramirez-Marquez, "A review of definitions and measures of system resilience," *Rel. Eng. Syst. Saf.*, vol. 145, pp. 47–61, Jan. 2016.

[17] C. Nan and G. Sansavini, "A quantitative method for assessing resilience of interdependent infrastructures," *Rel. Eng. Syst. Saf.*, vol. 157, pp. 35–53, Jan. 2017.

[18] C.-H. Wang and J. M. Blackmore, "Resilience concepts for water resource systems," *J. Water Resour. Planning Manage.*, vol. 135, no. 6, pp. 528–536, Nov. 2009.

[19] S. Shin *et al.*, "A systematic review of quantitative resilience measures for water infrastructure systems," *Water*, vol. 10, no. 2, pp. 1–25, 2018.

[20] P. Khatavkar and L. W. Mays, "Resilience of water distribution systems during real-time operations under limited water and/or energy availability conditions," *J. Water Resour. Planning Manage.*, vol. 145, no. 10, Oct. 2019, Art. no. 04019045.

[21] Y. Wang, C. Chen, J. Wang, and R. Baldick, "Research on resilience of power systems under natural disasters—A review," *IEEE Trans. Power Syst.*, vol. 31, no. 2, pp. 1604–1613, Mar. 2016.

[22] A. Gholami, T. Shekari, M. H. Amirioun, F. Aminifar, M. H. Amini, and A. Sargolzaei, "Toward a consensus on the definition and taxonomy of power system resilience," *IEEE Access*, vol. 6, pp. 32035–32053, Jun. 2018.

[23] N. Bhusal, M. Abdelmalak, M. Kamruzzaman, and M. Benidris, "Power system resilience: Current practices, challenges, and future directions," *IEEE Access*, vol. 8, pp. 18064–18086, Jan. 2020.

[24] M. Panteli, P. Mancarella, D. N. Trakas, E. Kyriakides, and N. D. Hatziargyriou, "Metrics and quantification of operational and infrastructure resilience in power systems," *IEEE Trans. Power Syst.*, vol. 32, no. 6, pp. 4732–4742, Nov. 2017.

[25] M. Panteli, C. Pickering, S. Wilkinson, R. Dawson, and P. Mancarella, "Power system resilience to extreme weather: Fragility modeling, probabilistic impact assessment, and adaptation measures," *IEEE Trans. Power Syst.*, vol. 32, no. 5, pp. 3747–3757, Sep. 2017.

[26] M. Panteli and P. Mancarella, "The grid: Stronger, bigger, smarter?: Presenting a conceptual framework of power system resilience," *IEEE Power Energy Mag.*, vol. 13, no. 3, pp. 58–66, May 2015.

[27] S. Zuloaga and V. Vittal, "Metrics for use in quantifying power system resilience with water-energy nexus considerations: Mathematical formulation and case study," in *Proc. IEEE Power Energy Soc. Gen. Meeting*, Aug. 2019, pp. 1–5.

[28] S. Zuloaga, P. Khatavkar, L. Mays, and V. Vittal, "Resilience of cyber-enabled electrical energy and water distribution systems considering infrastructural robustness under conditions of limited water and/or energy availability," *IEEE Trans. Eng. Manag.*, early access, Sep. 18, 2019, doi: 10.1109/TEM.2019.2937728.

[29] *ERCOT Planning Guide*, ERCOT, Austin, TX, USA, Jan. 2020.

[30] V. S. Y. Kwan, E. S. Naidu, and M. T. Bixter, "Controlling environmental crisis appraisal through knowledge, vividness, and timing," *J. Environ. Psychol.*, vol. 61, pp. 93–100, Feb. 2019.

[31] N. Y. Aydin, L. Mays, and T. Schmitt, "Sustainability assessment of urban water distribution systems," *Water Resour. Manage.*, vol. 28, no. 12, pp. 4373–4384, Jul. 2014.

[32] E. Bompard, R. Napoli, and F. Xue, "Analysis of structural vulnerabilities in power transmission grids," *Int. J. Crit. Infrastruct. Protection*, vol. 2, nos. 1–2, pp. 5–12, May 2009.

[33] E. Bompard, E. Pons, and D. Wu, "Analysis of the structural vulnerability of the interconnected power grid of continental europe with the integrated power system and unified power system based on extended topological approach," *Int. Trans. Electr. Energy Syst.*, vol. 23, no. 5, pp. 620–637, Jul. 2013.

[34] *Electric Power Monthly: With Data for July 2019*, U.S. Energy Inf. Agency, Washington, DC, USA, Sep. 2019.

[35] Illinois Center for a Smarter Electric Grid. (2018). *IEEE 14-Bus System*. [Online]. Available: http://icseg.iti.illinois.edu/ieee-14-bus-system

[36] *Recommended Electrical Network Design for Efficient Plant and Energy Operations*, Schneider Electr., Rueil-Malmaison, France, 2012.

[37] C. Grigg *et al.*, "The IEEE reliability test system-1996," *IEEE Trans. Power Syst.*, vol. 14, no. 3, pp. 1010–1020, Aug. 1999.

[38] S. Zuloaga, P. Khatavkar, V. Vittal, and L. W. Mays, "Interdependent electric and water infrastructure modelling, optimisation and control," *IET Energy Syst. Integr.*, vol. 2, no. 1, pp. 9–21, Mar. 2020.

SCOTT ZULOAGA (Member, IEEE) received the B.S.E and Ph.D. degrees in electrical engineering from Arizona State University, Tempe, AZ, USA, in May 2015 and 2020, respectively. He is currently a Planning Engineer with the Dynamic Studies Group, Electric Reliability Council of Texas.

VIJAY VITTAL (Life Fellow, IEEE) received the B.E. degree in electrical engineering from the B.M.S. College of Engineering, Bangalore, India, in 1977, the M.Tech. degree from the Indian Institute of Technology, Kanpur, India, in 1979, and the Ph.D. degree from Iowa State University, Ames, in 1982.

From 2005 to 2020, he was the Director of the Power System Engineering Research Center (PSERC). He is currently a Regents' Professor and the Ira A. Fulton Chair Professor with the Department of Electrical, Computer, and Energy Engineering, Arizona State University, Tempe, AZ, USA.

Dr. Vittal is a member of the National Academy of Engineering.